

Static scaling in a short-range Ising spin glass

K. Gunnarsson, P. Svedlindh, P. Nordblad, and L. Lundgren

Uppsala University, Department of Technology, Box 534, S-751 21 Uppsala, Sweden

H. Aruga and A. Ito

Ochanomizu University, Department of Physics, Faculty of Science, Bunkyo-ku, Tokyo 112, Japan

(Received 22 May 1990; revised manuscript received 29 November 1990)

The nonlinear ac susceptibility χ'_{nl} of the short-range Ising spin glass $\text{Fe}_{0.5}\text{Mn}_{0.5}\text{TiO}_3$ has been measured using a superconducting-quantum-interference-device magnetometer. The spin-glass temperature, T_g , and the critical exponent γ were estimated from the temperature dependence of the quadratic field term of χ'_{nl} , yielding $T_g=20.70$ and $\gamma=4.0$. Static-scaling analyses, using different scaling equations, gave similar results. Using γ and results from previous dynamic-scaling analyses, a number of critical exponents have been obtained through different scaling relations, e.g., $\delta=8.4$ and $\nu=1.7$. The results support the existence of a finite-temperature phase transition in a three-dimensional Ising spin glass.

The question whether the spin-glass transition is a true phase transition or a gradual freezing of the magnetic moments has been discussed during two decades of research. To describe critical phenomena in magnetic systems, the Ising model has played a major part. Concerning Ising spin-glass systems, no analytical solution to the problem exists. However, utilizing Ising models, both Monte Carlo (MC) simulations¹ and high-temperature series expansions² give strong indications of a phase transition at a finite temperature. Therefore, comparative studies on spin-glass materials that closely image a 3D Ising model system are of utmost importance to shed realistic light on this problem.

The magnetization in a spin-glass system may be expressed in odd powers of the magnetizing field, H :

$$M = \chi_0 H + \chi_2 H^3 + \chi_4 H^5 + \chi_6 H^7 + \dots \quad (1)$$

If a phase transition occurs at a finite temperature, T_g , the linear susceptibility term χ_0 is nondivergent, whereas the cubic term χ_2 and higher-order terms diverge in the critical region.^{3,4} Thus, to investigate a possible critical behavior in a spin glass, the adequate quantity to measure is the nonlinear susceptibility, χ_{nl} , defined as follows:

$$\chi_{nl} = \chi_0 - \frac{M}{H} \quad (2)$$

The response to an applied time varying magnetic field, $H = H_0 + h \sin \omega t$, where ω is the angular frequency, can be calculated using Eq. (1). For $h/H_0 \ll 1$, the amplitude of the ac component of the magnetization M_ω can be written:⁵

$$M_\omega = \chi_0 h + 3\chi_2 H_0^2 h + 5\chi_4 H_0^4 h + 7\chi_6 H_0^6 h + \dots \quad (3)$$

Differentiating with respect to the time varying field gives

$$\chi'(\omega) = \partial M_\omega / \partial h = \chi_0 + 3\chi_2 H_0^2 + 5\chi_4 H_0^4 + 7\chi_6 H_0^6 + \dots \quad (4)$$

In accordance with Eq. (2), we define the nonlinear ac susceptibility χ'_{nl} as

$$\chi'_{nl} = \chi_0 - \frac{\partial M_\omega}{\partial h} \quad (5)$$

In the low-field limit ($H_0 \rightarrow 0$), χ_2 always dominates χ'_{nl} . With increasing field the influence of higher-order terms becomes significant, and a deviation from an H_0^2 dependence will be observed. As the temperature approaches T_g , this deviation begins at continuously lower fields.

In this paper we present measurements of the nonlinear ac susceptibility of the short-range Ising spin-glass $\text{Fe}_{0.5}\text{Mn}_{0.5}\text{TiO}_3$. Static- and dynamic-scaling analyses in the vicinity of T_g yields good scaling behaviors with consistent values of the critical exponents and support the existence of a phase transition at a finite temperature. Comparisons are made with results from MC simulations on a 3D short-range Ising spin-glass system.¹

The magnetic structure of $\text{Fe}_{0.5}\text{Mn}_{0.5}\text{TiO}_3$ is most conveniently described by a hexagonal unit cell, with the spins aligned along the c axis. The spin-glass behavior is due to a random mixture of ferro and antiferromagnetic interactions within the hexagonal layers, causing bond disorder. The compound is regarded as a good model system for a 3D Ising spin glass.^{6,7} The sample used in this study was a single crystal in the shape of a rectangular parallelepiped, $2 \times 2 \times 5 \text{ mm}^3$, with its long axis parallel to the c axis.

The ac susceptibility measurements were made, using a superconducting-quantum-interference-device (SQUID) magnetometer, with a small ac field superimposed on a static field and both fields applied along the c axis of the crystal. The frequency of the ac field, $\omega/2\pi$, was either 1.7 Hz or 0.01 Hz. The ac magnetizing coil was wound directly onto the sample, which was glued on a sapphire rod and placed into a third-order gradiometer connected to the signal coil of the SQUID. In order to improve the resolution of the measurement, a second coil was wound

on the sapphire rod and centered in another section of the gradiometer to compensate out most of the influence of χ_0 on the measured signal. The components of the ac susceptibility, $\chi'(\omega)$ and $\chi''(\omega)$, were simultaneously detected by a PAR 5204 lock-in amplifier ($\omega/2\pi=1.7$ Hz) or a digital lock-in amplifier ($\omega/2\pi=0.01$ Hz). The signal-to-noise ratios $[\Delta\chi(\omega)/\chi(\omega)]$ were 5×10^{-5} ($\omega/2\pi=1.7$ Hz) and 1×10^{-4} ($\omega/2\pi=0.01$ Hz), respectively. The temperature was varied within the range $20.6 \text{ K} < T < 23.4 \text{ K}$. χ'_{nl} was measured as a function of increasing field, $2 \text{ G} < H_0 < 100 \text{ G}$, at a constant temperature. The magnitude of the ac field was kept at a constant value of 0.1 G throughout the experiment, ensuring the condition of $h/H_0 \ll 1$.

Figure 1(a) shows $\chi'(\omega)$ vs temperature for two different frequencies of the ac field and with $H_0=0 \text{ G}$ (open symbols) and $H_0=20 \text{ G}$ (solid symbols). Also indicated is the field-cooled (FC) susceptibility, χ_{FC} (triangles). The FC curve was obtained by stepwise cooling the

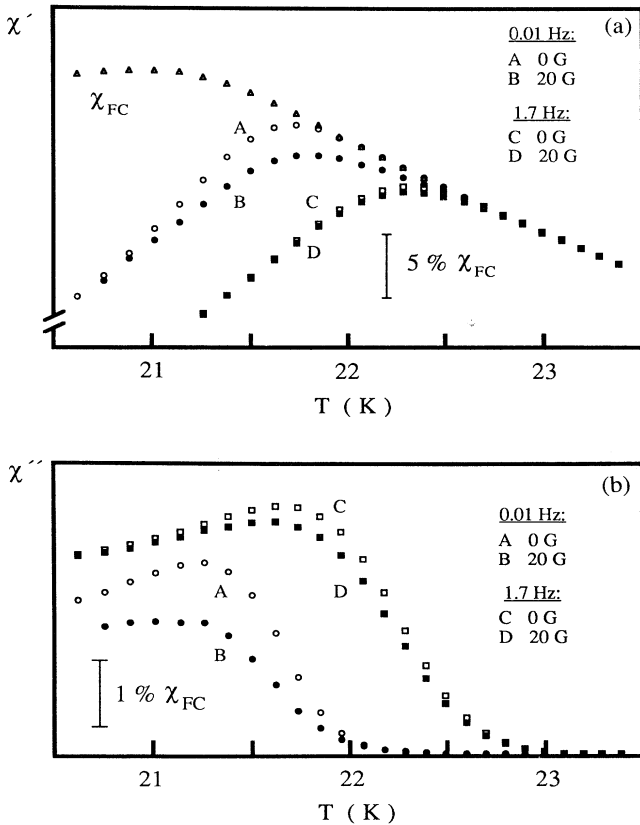


FIG. 1. The real part, $\chi'(\omega)$, and imaginary part, $\chi''(\omega)$, of the ac susceptibility vs temperature. The circles and squares correspond to two different frequencies of the ac field, $\omega/2\pi=0.01$ Hz and $\omega/2\pi=1.7$ Hz, respectively, ($h=0.1 \text{ G}$). The solid symbols mark a superposed static field $H_0=20 \text{ G}$, the open, $H_0=0 \text{ G}$. $T_g=20.70 \text{ K}$. (a) $\chi'(\omega)$ and FC susceptibility, $\chi_{FC}(H_0=1 \text{ G})$, vs temperature. 5% of the value of χ_{FC} at T_g is indicated. (b) $\chi''(\omega)$ vs temperature. 1% of the value of χ_{FC} at T_g is indicated.

sample in a small static field, $H_0=1 \text{ G}$. At each temperature, $T > T_g$, the slow spin-glass dynamics is characterized by a maximum relaxation time, τ_{max} . The FC susceptibility probes the equilibrium susceptibility, χ_{eq} , only when the time at constant temperature is longer than τ_{max} . Here, the temperature decrement was 0.1 K and the time at constant temperature 1000 s . According to previous zero-field-cooled (ZFC) magnetization measurements on the same sample,⁸ $\tau_{max} \approx 1000 \text{ s}$ at 21.4 K . Hence, at all temperatures above 21.4 K , χ_{FC} equals χ_{eq} . The $\chi'(\omega)$ curves in Fig. 1(a) deviate from the FC curve and exhibit cusps at certain temperatures, $T_f(\omega)$, which decrease with decreasing frequency. Consulting this figure, it is seen that the curves using the frequencies 0.01 and 1.7 Hz start to deviate from the equilibrium susceptibility below 22.0 K and 22.9 K , respectively. Below these temperatures, dynamic effects contribute to the measured nonlinear susceptibilities and the data *cannot be used* in analyses of the static critical behavior. In Fig. 1(b), the imaginary part of the ac susceptibility, $\chi''(\omega)$, vs temperature is visualized. In zero field, the inflection point of the $\chi''(\omega)$ curve is located at nearly the same temperature as the cusp of the corresponding $\chi'(\omega)$ curve. The suppression of $\chi''(\omega)$ with increasing field is striking.

Figure 2 displays $\log_{10}(\chi'_{nl}/\chi_{FC})$ vs $\log_{10}(H_0)$ at some different temperatures above T_g ($=20.70 \text{ K}$). The data at temperatures $1.067 < T/T_g < 1.097$ (open symbols) and $1.116 < T/T_g < 1.211$ (solid symbols) originate from measurements using $\omega/2\pi=0.01$ Hz and $\omega/2\pi=1.7$ Hz, respectively. According to the discussion above, χ'_{nl} should, in the low-field limit, have a quadratic dependence on H_0 , since χ_2 is the leading term. As can be seen in the figure, this is indeed the case. Only at the lowest temperature ($1.067 T_g$), a clear deviation from pure H_0^2 behavior is noticed. A more pronounced deviation is always anticipated at higher fields and/or lower temperatures.

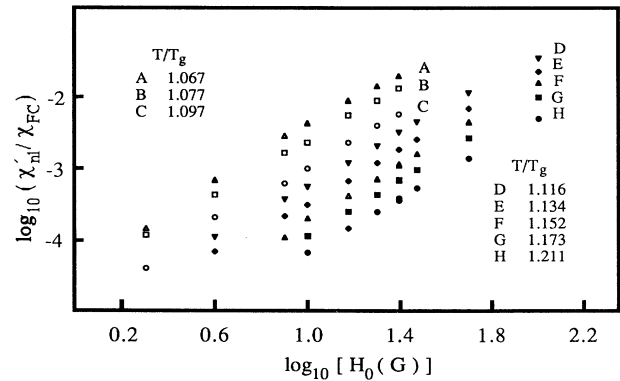


FIG. 2. $\log_{10}(\chi'_{nl}/\chi_{FC})$ vs $\log_{10}(H_0)$ at different temperatures within the range $1.067 < T/T_g < 1.211$. The curves corresponding to the three lower temperatures (open symbols) were obtained from ac susceptibility measurements using $\omega/2\pi=0.01$ Hz, the other curves (solid symbols) from measurements using $\omega/2\pi=1.7$ Hz.

Close to T_g , the coefficient of the H_0^2 term, χ_2 , is expected to diverge according to the critical scaling law:^{4,9}

$$\chi_2 \propto t^{-\gamma}, \quad (6)$$

where t is the reduced temperature $[(T/T_g)-1]$ and γ is a critical exponent. $\chi_2(T)$ was deduced from the initial slopes of χ'_{nl} vs H_0^2 plots. These values of χ_2 are displayed in Fig. 3, showing $\log_{10}(-\chi_2)$ vs $\log_{10}(t)$ for three different choices of T_g . The best straight line is obtained for $T_g = 20.70 \pm 0.20$ K, giving $\gamma = 4.0 \pm 0.3$. This value of T_g is close to the cusp temperature of the FC curve shown in Fig. 1(a). To describe χ_{nl} in the critical region, the following scaling equation has been proposed:⁴

$$\chi_{nl} = t^\beta G(H_0^2/t^{\beta+\gamma}). \quad (7)$$

$G(x)$ is a scaling function and β is the critical exponent of the spin-glass order parameter. $G(x)$ is linear for small x ; i.e., in the region where $\chi'_{nl} \propto H_0^2$. For $x \rightarrow \infty$, $G(x) \rightarrow x^{1/\delta}$, where δ is a critical exponent. A scaling plot of χ'_{nl} according to Eq. (7) is displayed in Fig. 4. The figure shows $\log_{10}(\chi'_{nl}/t^\beta)$ vs $\log_{10}(H_0^2/t^{\beta+\gamma})$, using $T_g = 20.70$ K, $\gamma = 4.0$, and $\beta = 0.54$, yielding a good data collapsing.

Using data from ac susceptibility measurements on the same sample, covering eight decades of frequency,¹⁰ β and T_g have earlier been estimated from dynamic-scaling analyses.¹¹ The parameters extracted were $z\nu = 9.5$, $\beta = 0.7$, and $T_g = 20.95$ K. Recently, a new approach to dynamic scaling has been proposed by Geschwind, Huse, and Devlin (GHD),¹² where $[\chi''(T, \omega)T] \omega^{-\beta/z\nu}$ is scaled

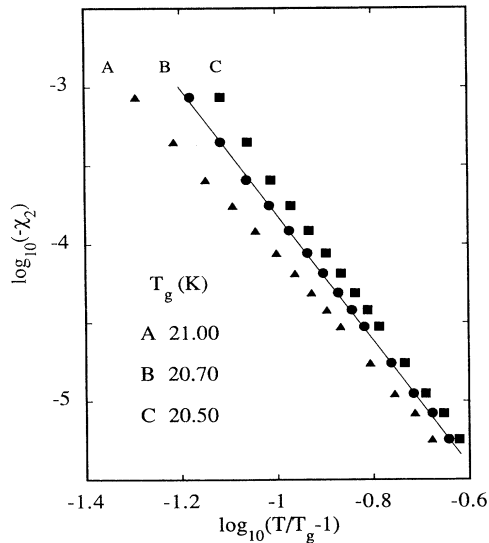


FIG. 3. $\log_{10}(-\chi_2)$ vs $\log_{10}(t)$ for three different values of T_g . The best fit, indicated by a solid line, is obtained for $T_g = 20.70$ K, yielding $\gamma = 4.0$.

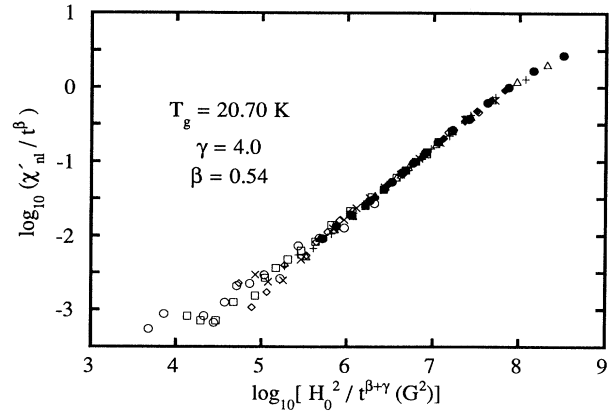


FIG. 4. $\log_{10}(\chi'_{nl}/t^\beta)$ vs $\log_{10}(H_0^2/t^{\beta+\gamma})$. The figure shows the data collapsing obtained using $T_g = 20.70$ K, $\gamma = 4.0$, and $\beta = 0.54$.

vs $t/\omega^{1/z\nu}$, providing the possibility to make linear scaling plots. In a logarithmic graph, all values are given equal weight, despite the fact that small values, generally, are less accurate. Since both $\beta/z\nu$ and $1/z\nu$ typically are of order 0.1, the new approach provides a linear scaling plot where the experimental error can be included. GHD also suggest a method for separate estimation of the ratio $\beta/z\nu$ through scaling of the peak values in $\chi''(T, \omega)$ vs T for different frequencies, which for our data gives $\beta/z\nu = 0.051 \pm 0.005$. Keeping this value of $\beta/z\nu$ and using $T_g = 20.70$ (Fig. 3), the best data collapsing according to this new dynamic-scaling approach is achieved for $z\nu = 10.5 \pm 1.0$. However, it should be noticed that lower values of T_g (≈ 20.5 K), with correspondingly higher values of $z\nu$, will result in equally good data collapsing. The reason for achieving different values of the critical exponents and T_g in these two approaches to dynamic scaling is not completely understood. In general, it is important to take into account the nonequilibrium character of $\chi''(\omega)$ within the critical region.¹³ The time dependence of $\chi''(\omega)$ will make results from scaling analyses less reliable. Considering the best fit to $\log_{10}(-\chi_2)$ vs $\log_{10}(t)$ and the outcome from dynamic scaling cited above, we regard $T_g = 20.70 \pm 0.20$ K as a reasonable result.

Since the results presented in this paper on the non-linear susceptibility are low-field data, where χ_2 dominates, the influence of β on the static-scaling plots of χ'_{nl} is weak. In order to accurately determine the value of β from static-scaling plots, measurements must also be performed in higher fields or in the limit $t \rightarrow 0$. As evident from the discussion above, $t \rightarrow 0$ would require measurements in the ultralow frequency region to guarantee dynamic equilibrium. Guided by the results above, we henceforth put $\beta = 0.54$ in our analyses of χ'_{nl} . In general, it is valuable to find methods to separately estimate the different scaling parameters. Only making the complete scaling plots, it is almost impossible to find *one unique set of values*, satisfying the condition of best data

collapsing. For instance, $T_g = 20.5$ K, $\gamma = 4.3$, and $\beta = 0.56$ or $T_g = 20.95$ K, $\gamma = 3.60$ and $\beta = 0.7$, will give equally good data collapsing as the one in Fig. 4.

As has been mentioned above, a logarithmic scaling plot gives equal weight to all values of χ'_{nl} , although the smaller values often are less accurate. In the present case, this is to some extent balanced by the better resolution of the measurements at $\omega/2\pi = 1.7$ Hz, used for temperatures above $1.116 T_g$. In order to better consider the experimental error, a new static-scaling equation has recently been proposed by Geschwind *et al.*:¹⁴

$$\chi_{nl} \propto H_0^{2\beta/(\gamma+\beta)} \underline{G}(t/H_0^{2/(\beta+\gamma)}) \quad (8)$$

where $\underline{G}(x)$ is a scaling function, and $\underline{G}(x) \rightarrow 1$ for $x \rightarrow 0$ and $\underline{G}(x) = x^{-\gamma}$ in the region where $\chi'_{nl} \propto H_0^2$. Using Eq. (8), it is possible to make a linear scaling plot of the data from Fig. 4. Figure 5 shows a scaling plot of $\chi'_{nl}/H_0^{2\beta/(\gamma+\beta)}$ vs $t/H_0^{2/(\gamma+\beta)}$ using $T_g = 20.70$ K, $\gamma = 4.0$, and $\beta = 0.54$, yielding a good data collapsing. Since the values of $2\beta/(\gamma+\beta)$ and $2/(\gamma+\beta)$ are 0.3 and 0.15, respectively, the H_0 dependence of the scaling plot is weak and the curve resembles χ'_{nl} vs T . The exact value of the exponent β has only a minor influence on the quality of the data collapsing. Also, similar to static scaling according to Eq. (7), it is impossible to find a unique set of parameters that gives the ultimate data collapsing. If there was no guidance from our separate estimate of T_g and γ from $\chi_2(T)$, e.g., $T_g = 20.5$ K, $\gamma = 4.3$, and $\beta = 0.56$ or $T_g = 20.95$ K, $\gamma = 3.60$, and $\beta = 0.7$ would give a comparably good data collapsing.

A number of estimates of γ has been reported^{15,16} forming a wide interval of values, $\gamma = 4.0$ being among the highest. One possible reason for achieving a too low value of γ is by using a too high value of T_g in Eq. (6), e.g., Fig. 3, curve A. MC simulations on a 3D Ising system¹ have given $\gamma = 2.9 \pm 0.1$. In those simulations the average correlation time, τ_{av} , was derived from the decay of the spin correlation function $\langle s(0)s(t) \rangle$, measured during $10^0 - 10^8$ MC steps. T_g was then calculated through power-law scaling of τ_{av} in the range $1.1 < T/T_g < 2.0$. However, this temperature interval is likely to be out of the critical region and corrections to conventional dynamic scaling are then needed¹ to estimate the true value of γ .

From our values of the critical exponents, $\gamma = 4.0$ and $\beta = 0.54$, it is possible to calculate related critical exponents. The exponent δ is derived from $\delta = \gamma/\beta + 1 = 8.4 \pm 1.5$. Values of the same order of magnitude have been reported earlier,² although reports of smaller values are in the majority. MC simulations¹ have given $\delta = 6.8 \pm 1.2$. The specific-heat exponent is given by the relation $\alpha = 2 - 2\beta - \gamma$, yielding $\alpha = -3.1$. Since the specific heat scales as $t^{-\alpha}$, no divergence at T_g should be observed, in accordance with experimental results on spin glasses.¹⁷ Further, the correlation length of the spin-glass order parameter scales as follows: $\xi \propto t^{-\nu}$. The exponent may be derived from $\nu = (2 - \alpha)/d$, where d is the spatial dimension. The result is $\nu = 1.7$. Compared to the value obtained from MC simulations on a Ising spin-glass system,¹ $\nu = 1.3 \pm 0.1$, our value is significantly higher.

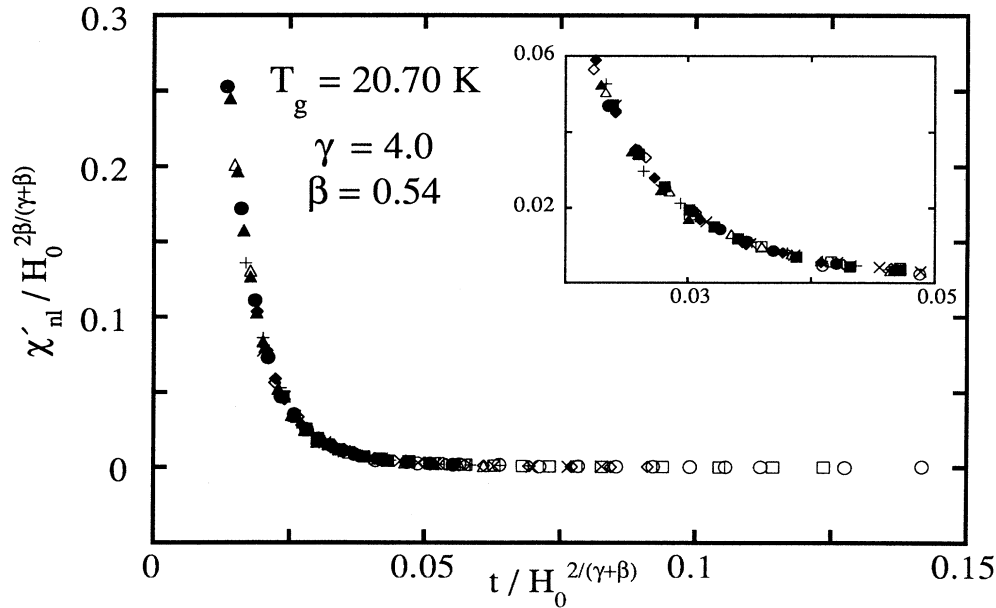


FIG. 5. $\chi'_{nl}/H_0^{2\beta/(\gamma+\beta)}$ vs $t/H_0^{2/(\gamma+\beta)}$. The figure shows the data collapsing obtained using $T_g = 20.70$ K, $\gamma = 4.0$, and $\beta = 0.54$. The insert figure displays a magnified part of the plot.

From ν and γ it is possible to calculate η , governing the long-distance behavior of the spatial correlation function at T_g ; $\eta=2-(\gamma/\nu)=-0.35$. The result from simulations is $\eta=-0.22$.¹ Finally, using $\nu=1.7$ and $z\nu=10.5$, z is equal to 6.2, which is in good agreement with both MC results¹ ($z=6.0\pm 0.5$) and values from other measurements reported, e.g., $z=5.3\pm 0.8$ (Ref. 2) from measurements on a Ruderman-Kittel-Kasuya-Yosida (RKKY) spin glass.

The outcome of our analyses of the nonlinear susceptibility of $\text{Fe}_{0.5}\text{Mn}_{0.5}\text{TiO}_3$ supports the existence of a phase transition at T_g . The best fit of the H_0^2 term of χ'_{nl} according to Eq. (6) yields $\gamma=4.0\pm 0.3$ for $T_g=20.70\pm 0.20$ K. Static scaling according to two different scaling equations, Eqs. (7) and (8), give good data collapsing in the critical region using the same set of parameters; $\gamma=4.0$,

$\beta=0.54$, and $T_g=20.70$ K. The values of the extracted critical exponents should be representative for 3D Ising spin glasses in general. Previous dynamic-scaling analysis yields $T_g=20.95$ K, while a new approach to dynamic scaling suggests T_g to be lower, viz. $T_g=20.70$ K. The reason for obtaining different values of the spin-glass critical temperature and the critical exponents using different approaches to dynamic scaling is not fully understood. One reason may be not taking into account the nonequilibrium character of the quantity scaled within the critical region.¹³ The time dependence of $\chi''(\omega)$ in the vicinity of (and below) T_g will be further investigated.

Financial support from the Swedish Natural Science Research Council (NFR) is gratefully acknowledged.

¹A. T. Ogielski, Phys. Rev. B **32**, 7384 (1985).

²R. Singh and S. Chakravarty, J. Appl. Phys. **61**, 4095 (1987).

³J. Chalupa, Solid State Commun. **24**, 429 (1977).

⁴M. Suzuki, Prog. Theor. Phys. **58**, 1151 (1977).

⁵L. Lévy, Phys. Rev. B **38**, 4963 (1987).

⁶A. Ito, H. Aruga, E. Torikai, M. Kikuchi, Y. Syono, and H. Takei, Phys. Rev. Lett. **57**, 483 (1986).

⁷A. Ito, H. Aruga, M. Kikuchi, Y. Syono, and H. Takei, Solid State Commun. **66**, 475 (1988).

⁸P. Svedlindh, K. Gunnarsson, P. Nordblad, L. Lundgren, H. Aruga, and A. Ito, J. Magn. Magn. Mater. **71**, 22 (1987).

⁹S. Katsura, Prog. Theor. Phys. **55**, 1049 (1976); A. Aharony and Y. Imry, Solid State Commun. **20**, 899 (1976); J. Chalupa, Solid State Commun. **22**, 315 (1977).

¹⁰K. Gunnarsson, P. Svedlindh, P. Nordblad, L. Lundgren, H.

Aruga, and A. Ito, Phys. Rev. Lett. **61**, 754 (1988).

¹¹P. Nordblad, L. Lundgren, P. Svedlindh, K. Gunnarsson, H. Aruga, and A. Ito, J. Phys. (Paris) **C8**, 1069 (1988).

¹²S. Geschwind, D. A. Huse, and G. E. Devlin, Phys. Rev. B **41**, 4854 (1990).

¹³L. Lundgren, P. Svedlindh, and O. Beckman, J. Magn. Magn. Mater. **31-34**, 1349 (1983).

¹⁴S. Geschwind, D. A. Huse, and G. E. Devlin, Phys. Rev. B **41**, 2650 (1990).

¹⁵H. Bouchiat, J. Phys. (Paris) **47**, 71 (1986).

¹⁶P. Svedlindh, L. Lundgren, P. Nordblad, and H. S. Chen, Europhys. Lett. **2**, 805 (1986).

¹⁷G. E. Brodale, R. A. Fisher, W. E. Fogle, J. O. Phillips, and J. van Curen, J. Magn. Magn. Mater. **31-34**, 1331 (1983).